B. PROJECT SUMMARY

Overview: Stroke, Parkinson's disease, and osteoarthritis affect roughly 15% of the U.S. adult population and often impair walking ability, leading to an increased risk of serious health conditions (e.g., heart disease, diabetes, high blood pressure, obesity) and a decreased quality of life. Traditional approaches for assessing patient function and delivering rehabilitation prescriptions require that the patient make repeated visits to the clinic, which is expensive and time consuming for the patient, the clinician, and the health care system. Ideally, clinicians would be able to gather quantitative information about patient walking function, as well as deliver rehabilitation prescriptions that improve patient walking ability, when the patient is at home or in the community. While the advent of inexpensive wearable technology such as wireless inertial measurement units (IMUs) could make remote assessment of function and remote delivery of treatment a possibility, such capabilities have not yet become a reality.

Given that numerous companies now market relatively low cost IMU-based human motion measurement systems, why haven't these systems become ubiquitous for clinical use, both inside and outside clinical and laboratory environments? The problem is not with the hardware – the problem is with the software that turns IMU data into joint kinematic data. That being the case, what does the software need to do for IMU-based motion measurement systems to achieve widespread clinical utilization?

1) The software should require data from as few IMUs as possible to make IMU attachment to the body segments fast, easy, and repeatable.
2) The software should be able to calibrate patient-specific kinematic models automatically, rapidly, and with minimal effort.
3) The software should provide joint motion measurements of comparable accuracy to those available from marker-based motion capture systems.
4) The software should be fast and flexible enough to support both off-line data logging and real-time feedback applications.
5) The software should be so easy to use that any patient, family member, or caregiver can use it anywhere – indoors or outdoors - with no technical expertise and minimal training.

The objective of this proposal is to develop novel software that achieves these goals without requiring magnetometer data that is susceptible to the presence of metal in the test environment. The proposed software will combine several novel computational ideas to convert IMU accelerometer and gyroscope data into accurate joint kinematic data. The proposed project will 1) DEVELOP the necessary computational algorithm using pre-existing IMU- and marker-based motion capture data collected simultaneously, 2) EVALUATE the algorithm's ease of use and accuracy by having 10 healthy subjects collect their own IMU-based motion capture data, and 3) DEPLOY the algorithm on a Windows tablet to demonstrate that it can be used for real-time feedback applications.

Intellectual Merit: The intellectual merit of the proposed project involves the development of novel computational approaches that lead to _more accurate_ joint kinematic measurements using _fewer_ IMUs than with existing methods. These approaches take advantage of joint constraints in kinematic models, use _measured_ and _differentiated_ IMU data in addition to commonly used _integrated_ IMU data, and include a potentially more accurate way to numerically integrate IMU linear acceleration data.

Broader Impacts: If successful, this project could have wide-reaching benefits to the field, society, and education. For the field, human motion measurement could be moved outside the laboratory environment, allowing fast, easy, accurate, and inexpensive measurements to be made under uncontrolled real-life conditions. For society, remote real-time measurement of human motion could facilitate the development of effective remote monitoring and telerehabilitation methods that reduce the need for clinician time and patient office visits, resulting in a reduced cost to the healthcare system. For education, "at risk" middle school students from underrepresented groups will experience first-hand ways that IMU technology is being used to improve human health, encouraging them to pursue a college education in a STEM-related field.

D. PROJECT DESCRIPTION

I. Objectives and Significance

When the human neuromusculoskeletal system is impaired, mobility is often limited, leading to an increased risk of associated health conditions (e.g., heart disease, diabetes, high blood pressure, obesity)[1] and a decreased quality of life[2]. Common clinical examples include osteoarthritis, stroke, and Parkinson's disease, which together affect roughly 15% of the U.S. adult population[3–5]. Because the extent and characteristics of impairment vary from individual to individual, customized rehabilitation approaches are needed to address this important societal problem.

Currently, assessment of patient function and delivery of rehabilitation prescriptions must be done in a clinical or laboratory setting. Furthermore, treatment delivery typically involves the clinician instructing the patient how to perform the desired movement pattern but without any quantitative feedback on performance. As a result, rehabilitation efficacy is often sub-optimal at restoring near-normal walking ability[6,7]. From a logistical perspective, patient assessment and treatment delivery require repeated visits to the clinic, putting a strain on the patient, the clinician, and the health care system. Furthermore, patient assessment performed in the clinic may not represent the patient's actual function in the community, where the environment is less controlled. Thus, the ability to monitor patient function and deliver rehabilitation prescriptions remotely, without clinician involvement, could improve quality of care while reducing the time and cost to the patient, the clinician, and the health care system.

To realize such capabilities, technological advances are required in the areas of functional assessment and treatment delivery. For functional assessment, ideally patient movement patterns could be measured remotely in a home or community environment using simple, easy-to-use technology. Ideally the technology would be so simple and easy to use that the patient or a family member/caregiver could collect the desired movement data and transfer it automatically to the clinician. For treatment delivery, providing quantitative feedback while also moving outside the clinic could result in more effective, easier logistically, and less costly interventions. A primary obstacle to achieving such changes is that the equipment commonly used for measuring human movement – an optical motion capture system – is extremely expensive (tens to hundreds of thousands of dollars), requires special training and knowledge to use, requires extensive setup for data collection, is typically available only in a research lab or clinic, and cannot be used outside of a calibrated indoor volume. Thus, **assessment of patient function and delivery of feedback-based rehabilitation prescriptions outside the clinic would be greatly facilitated by the development of a user-friendly human motion measurement system that is portable and provides both off-line data logging and real-time feedback of movement patterns.**

Inertial measurement units (IMUs) have emerged as the most promising technology for inexpensive, wireless, and portable measurement of human movement. IMUs typically contain three types of sensors: 1) an accelerometer that measures tri-axial linear acceleration, including the acceleration due to gravity, 2) a gyroscope that measures tri-axial angular velocity, and 3) a magnetometer that measures the direction of the Earth's magnetic field (typically the most unreliable measurement due to metallic disturbances in the surrounding environment). Each of these measurements is expressed in terms of axes fixed in the IMU, making it challenging to relate IMU measurements to Earth-fixed axes when the IMU is moving. While IMUs have great potential for reconstructing walking patterns outside the laboratory, little work has been performed to develop the theory, algorithms, and software needed to achieve this goal[8]. Most academic research to date has involved algorithms for using a single IMU to measure the motion of a single body segment. Though at least two companies (Xsens and APDM) have developed full-body IMU-based motion measurement systems[9,10], these systems are not simple or user-friendly enough to be used by patients or their caregivers outside the clinic. What is needed is a wireless IMU-based human motion measurement system that is so easy to use and user friendly that virtually any individual could use it in any environment with minimal instruction and set up.

The objective of this project is to develop a computational algorithm that makes it easy for minimally trained individuals with no technical expertise to use low-cost wireless IMUs to collect accurate full-body walking kinematics in any environment, thereby facilitating functional assessment and rehabilitation delivery outside the clinic. To make set up and use of an IMU system as simple as possible, our proposed algorithm will use a minimal number of IMUs that can be attached easily and repeatably to specified body

segments. Specifically, the proposed algorithm will require only 6 IMUs that can be easily-attached on the feet, the pelvis, the trunk, and the wrists, and will provide remote data logging and real-time feedback of walking kinematics. Since IMUs are relatively inexpensive, use of a minimum number is not for cost reasons but rather to make the system as simple to use as possible. Data collection will be controlled by a Windows tablet so that the system can be used by anyone, anywhere, and at any time. Pre-existing IMU- and marker-based motion capture data collected simultaneously from a subject performing walking and other motions will be used to facilitate the development of the proposed algorithm. Evaluation of the algorithm's ease of use and accuracy will involve testing 10 healthy subjects who will put on the IMUs themselves after reviewing a training worksheet and/or video, with marker-based motion capture data being collected simultaneously for comparison of calculated joint kinematics. Deployment of the algorithm in a prototype IMU-based motion measurement system will be performed using a Windows tablet to demonstrate the algorithm's ability to calculate and display joint kinematics in real time using either Matlab animated plots or an OpenSim animated skeletal model.

II. Broader Impacts

The broader impacts of the proposed project relate to both research and education. For research, our proposed IMU-based human motion measurement algorithm could eventually make it possible to replace complicated and expensive optical motion capture systems that are limited to a controlled laboratory environment with a user-friendly inexpensive IMU-based motion capture system that is unlimited in where it can be used. Such a system could make it possible to perform remote assessment of patient function and remote delivery of rehabilitation prescriptions, where patients would don the IMUs and run the data collection and visualization process themselves, with their joint kinematics being transferred automatically to a clinician for review. This quantitative approach could increase treatment effectiveness while simultaneously decreasing the time, effort, and cost incurred by the patient, the clinician, and the healthcare system. These capabilities are the result of being able to omit IMUs from some body segments when still measuring full-body motion. Since our proposed algorithm estimates not only joint positions and velocities but also joint accelerations, with future developments it could potentially be used to estimate inverse dynamic joint loads without the use of force plates. Such capability would open the door to an even broader array of rehabilitation applications, such as those involving not only desired changes in joint motions but also desired changes in joint loads (e.g., gait modification to treat knee osteoarthritis). The algorithm could also potentially be valuable for military applications involving remote monitoring of soldier movements in the field of battle. For education, "at risk" students in a local middle school will interact with the technology first-hand by competing in an annual "Jump Off" competition held via Skype with students in a sister middle school in Auckland, New Zealand. In addition, the software and data developed for this project will be distributed to the academic community freely via the web so that other researchers can use it to expand the scope of remote assessment and remote rehabilitation applications.

III. Relation to Present State of Knowledge in the Field

This section summarizes the current state of knowledge in the use of IMUs for measuring human motion.

Historically, human motion measurement with IMUs has involved placing one IMU on every body segment, calculating the orientation of each segment separately using its attached IMU, and finally determining the relative orientation between adjacent segments to estimate joint angles. Calculation of body translations is normally omitted, since such calculations require double integration of IMU acceleration measurements, leading to numerical integration drift. Calculating motion for each segment independently produces kinematically inconsistent results where joints in a linked-segment kinematic model would fly apart. This situation is similar to one encountered previously by the PI when using linked-segment kinematic models to calculate joint angles from marker-based motion capture data[8,11].

For this reason, several recent studies that measured human movement with IMUs have incorporated joint constraints from linked-segment kinematic models into the solution process for estimating joint positions and velocities (Table 1). However, these studies used generic kinematic models where the positions/orientations of joint axes in the body segments were not numerically calibrated to subject movement data through some type of optimization procedure, as has been done by the PI and others for marker-based motion capture data[8,11]. For example, in Kortier *et al.*'s (2014)[12] study of hand kinematics

measured with IMUs, the authors reported that, "We have observed that the estimation accuracy strongly depends on the sensor to segment calibration procedure," and furthermore, that "Accurate determination of functional joint position . . . and the axis of rotation . . . would improve the accuracy."

Despite this limitation, recent studies have still achieved IMU kinematic measurement accuracy on a par with marker-based motion capture systems. For example, both El-Gohary and McNames (2012)[13] and Koning *et al*. (2015)[8] achieved root-mean-square (RMS) errors relative to a marker-based motion capture system on the order of 4 to 6 degrees. Such accuracies have been achieved primarily by using kinematic models with joint constraints, which reduce integration error accumulation by forcing integrated joint positions to remain consistent with the constraints in the underlying kinematic model, and by using novel methods to correct integration drift when a known situation is encountered (e.g., when the foot passes below ground level during walking).

Despite the increased use of kinematic constraint equations for estimating joint motions from IMU data, all of the recent studies in Table 1 used one IMU per body segment modeled, which complicates the IMU system setup and data collection process. Since joint constraints imposed by an underlying kinematic model reduce the number of model states that must be found, one IMU per body segment may be far more than necessary to achieve accurate joint motion measurements. In addition, only two of the studies below calculated translations of the base segment in the kinematic model, and none calculated joint accelerations, which would be useful for estimating joint loads via inverse dynamics. It is also noteworthy that only one study listed below, a white paper written by employees of Xsens Technologies in the Netherlands[9], estimated joint positions in real time, despite the fact that some form of the computationally efficient Kalman filtering method (discussed in greater detail below) was used in two of the studies. The Xsens method is also unique in that it enforces "soft" joint constraints, allowing the joints in their kinematic model to pull apart slightly based on specified tolerances.

Table 1: Summary of recent published studies that used IMUs to measure human movement. Abbreviations are: EKF = Extended Kalman filter; EMD = Empirical mode decomposition; UKF = Unscented Kalman filter; O = Optimization; DC = Direct calculation

Study	Anatomy Modeled	IMUs per Segment	Kinematic Constraints	Base Translation	State Estimation	Real Time	Drift Correction
Kortier et al. (2014) [12]	Hand	1	Yes	Yes	EKF	No	Yes
Bonnet et al. (2014) [14]	Trunk	1	No	No	EMD	No	Yes
El-Gohary & McNames (2012) [13]	Arm	1	Yes	No	UKF	No	Yes
Koning et al. (2015) [8]	Lower body	1	Yes	No	O	No	No
Roetenberg et al (2013) [9]	Full body	1	Yes*	Yes	EKF	Yes	Yes
Schiefer et al. (2014) [15]	Upper body	1	No	No	DC	No	Yes

One of the main technological developments for the proposed project will be a computational approach for predicting full-body human movement – including joint positions, velocities, *and accelerations* – outside the laboratory using a **minimal number** of IMUs and a model with joint constraints. Use of a minimal number of IMUs attached in a simple and repeatable manner would facilitate human motion measurement by patients or caregivers in non-clinical and non-research environments. We are unaware of any published studies that have explored the issue of how many IMUs are needed to obtain human movement measurements of comparable accuracy to that of an optical motion capture system. Furthermore, while studies are beginning to take advantage of kinematic model constraint equations to improve the accuracy of human motion measurement with IMUs, no studies are exploring how these equations impact the number of IMUs needed for accurate motion measurement, which in turn affects the simplicity and ease of use of any proposed IMU system.

IV. Work in Progress by the Principal Investigators

The proposed project builds naturally on four ongoing research efforts by the PI and co-PI related to human motion measurement using IMUs, providing a solid foundation for the project.

A. Unscented filter for marker-based motion measurement: For the first effort, the PI's lab has continued to explore the use of an unscented filter (UF, the nonlinear version of a Kalman filter) for performing inverse kinematic analyses using marker-based motion capture data[16]. The UF is an optimal estimator that combines the efficiency of the Kalman filter (KF) with the capabilities of the unscented transformation (UT), a method for determining the statistics of a random variable that undergoes a nonlinear transformation[17,18]. Given a random variable and its mean and covariance, a set of sigma points

is created based on the matrix square root decomposition of the covariance matrix. These points are propagated through the model equations, rather than propagating the random variable itself, and a new weighted mean and covariance of the variable are determined[17–20].

The UF uses the UT process to generate optimal *state* and *parameter* estimates, where a *state* is considered to be any time-varying quantity being estimated and a *parameter* is considered to be any constant quantity being estimated. Using a dynamic process model and the measurement equations associated with the model being calibrated, a set of measurement estimates, or *observations*, is created from the filter sigma points. These observations are compared to the experimental measurements each time a measurement becomes available. Based on the resulting error, the UF gain and covariance matrices are updated and the process is repeated to generate state estimates for the next iteration. As the error between observed and experimental measurements is minimized, the state estimates converge to their statistically optimal values[17–20]. While previous human movement studies have primarily used extended Kalman filters, we explored the UF because it has lower expected estimation error than other nonlinear filters, can be applied to non-differentiable functions, avoids the derivation of Jacobian matrices, and is valid for higher-order expansions than other nonlinear filters[21].

To evaluate the ability of a UF to estimate joint kinematics *and* model parameter values simultaneously from noisy surface marker data during walking, we previously used a 5 DOF version of the 6 DOF walking model shown in Fig. 1, where the foot segment was omitted[16]. We derived the non-linear marker position equations for the model using Autolev (MotionGenesis, Palo Alto, CA) and generated synthetic joint and marker motion data using joint kinematics taken from published walking data[22]. We added zero mean, Gaussian white noise to the model marker positions (standard deviation of 0.5 cm) to emulate the effect of skin motion artifacts. We used joint position, velocity, acceleration, and jerk as our model state to facilitate prediction of joint accelerations and implemented the entire UF solution process in Matlab.

As shown in Table 2 below, our UF algorithm successfully recovered joint motions and segment lengths from the noisy marker measurements. Joint position, velocity, *and* acceleration estimates and marker position estimates were in close agreement with the corresponding true time histories. In addition, segment lengths were estimated to within 1% of their true values. These results demonstrate the ability of UF methods to handle discontinuous and noisy measurements directly without data pre-processing. While the PI has extensive experience using optimization methods to calibrate joint and marker plate positions/orientations on the body segments of kinematic walking models[11,22–25], we will use an unscented filter for the proposed project due to its faster computational speed and its ability to handle real-time applications.

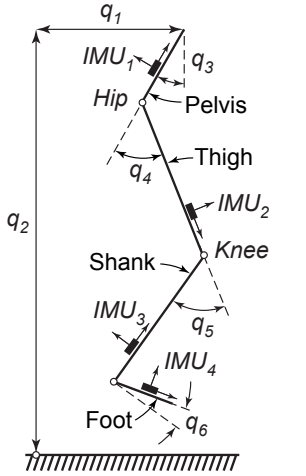

Fig. 1: Schematic of planar 6 DOF kinematic walking model used to demonstrate proposed IMU-based motion measurement method.

***2. Novel algorithm for IMU-based motion measurement*:** (This section contains confidential information that the University of Auckland requests not be released to persons outside the Government, except for purposes of review and evaluation.) For the second effort, PI Fregly and co-PI Besier recently developed a novel filter-based algorithm for converting IMU data provided by a minimal number of IMUs into joint kinematic data in multibody models of human movement. Dr. Besier is a co-founder of the New Zealand-based IMU company IMeasureU, which was recently acquired by Vicon Motion Systems and is pursuing IMU-based motion measurement applications in the athletic and human performance areas. The unique aspects of our proposed algorithm are that 1) it uses IMU data from the current time point to estimate kinematic model state at the current time point, thereby making use of the most up-to-date IMU data available rather than IMU data from the previous time point, 2) it uses all available IMU data in the state estimation process, including measured and differentiated IMU data in addition to standard integrated IMU data, and 3) it includes joint accelerations and not just joint positions and velocities in the state vector, allowing state estimates to be used directly for inverse dynamic analyses with additional differentiation. These unique aspects may make it possible to develop a simple and easy-to-use IMU-

Table 2: Average root-mean-square errors (Avg RMSE) and range of associated input data (Data Range - for comparison) for unscented filter inverse kinematics performed on a 5 DOF planar walking model using noisy synthetic marker data.

Errors	Avg RMSE	Data Range
Markers (m)	1.2e-6	1.5
Positions (m)	2.1e-4	1.1
Orientations (rad)	1.4e-3	0.5
Velocities (m/s)	3.8e-3	2.1
Angular Velocities (rad/s)	3.9e-2	3.3
Accelerations (m/s^2)	8.9e-2	9.5
Angular Accelerations (rad/s^2)	1.9	20.7

based human motion measurement system that can measure full-body walking motions accurately using only 6 IMUs that can be attached easily and repeatably by any user without extensive training.

To understand the benefits of the proposed algorithm, consider the following example problem and think in terms of number of equations and number of unknowns. The simplest problem that contains the necessary features is a planar 6 degree-of-freedom (DOF) walking model consisting of pelvis, thigh, shank, and foot segments (i.e., one leg only), where the pelvis possesses 3 DOFs relative to a laboratory coordinate system and the hip, knee, and ankle are modeled as 1 DOF pin joints (review Fig. 1). We will consider how data from either 4 IMUs (one per segment) or 2 IMUs (pelvis and foot segments only) could be used to calculate joint kinematics in the 6 DOF model (i.e., inverse kinematics) by following a "standard" method and our proposed method. The "standard" method is a "strapdown inertial navigation algorithm"[26] similar to the Xsens method[9] except that it uses rigid body joint constraints from the 6 DOF model and does not include "reality constraints" or additional data from a magnetometer, which could be added if desired. Both methods require distinguishing between experimental and model IMU data. While **experimental IMU data** represents quantities obtained from an actual IMU, **model IMU data** represents corresponding quantities calculated by the 6 DOF kinematic model using a guess for the model's joint kinematics. Furthermore, for experimental IMU data, the data can be categorized as either **measured** (meaning IMU angular velocities and linear accelerations measured by the sensor), **integrated** (meaning IMU orientations, linear velocities, and positions obtained by numerical integration), or **differentiated** (meaning IMU angular accelerations obtained by numerical differentiation). Model IMU data includes all three types of quantities.

To convert measured experimental IMU data into 6 DOF model joint kinematics, the standard method employs the following general process:

1) Numerically integrate measured experimental IMU data from time frame *i* using an explicit integration scheme to find integrated experimental IMU data at time frame *i*+1. Subtract the acceleration due to gravity from the experimental accelerations as part of this step.
2) Define joint positions and velocities in the 6 DOF model at time frame *i*+1 as the model state.
3) Find model state at time frame *i*+1 such that model IMU orientations, velocities, and positions match corresponding integrated experimental IMU quantities at time frame *i*+1 as closely as possible.
4) Replace integrated experimental IMU quantities at time frame *i*+1 with corresponding model IMU quantities to minimize the effect of integration drift and prepare for solving the next time frame.

Either an optimization or a Kalman filtering approach can be used to implement this process (Table 1).

In contrast to the standard method, **our proposed method uses integrated as well as measured and differentiated experimental IMU data at time frame *i*+1 to determine kinematic model state (including joint accelerations) at time frame *i*+1.** By making use of the most recent measured experimental IMU data and by enforcing numerical integration relationships between time frames *i* and *i*+1 as constraints, **our approach produces more highly overdetermined problems than with the standard method**. To convert measured experimental IMU data into 6 DOF model joint kinematics, the proposed method employs the following general process:

1) Numerically integrate measured experimental IMU data at time frame *i*+1 (rather than *i*) using an implicit (rather than explicit) numerical integration scheme to find integrated experimental IMU data at time frame *i*+1. We use an implicit integration scheme since we wish to utilize IMU data from the end of the interval and because implicit integration provides better numerical stability compared to explicit integration[27]. If desired to improve numerical accuracy, we could also use multistep integration with two or more past time frames of model IMU data. We also subtract the acceleration due to gravity from the experimental accelerations as part of this step.
2) Numerically differentiate measured experimental IMU angular velocity data at time frame *i*+1 using a backward finite difference relationship to estimate experimental IMU angular acceleration at time frame

i+1. Since IMU angular velocity is expressed in terms of unit vectors fixed in the IMU, IMU angular acceleration can be calculated by differentiating the scalar IMU angular velocity components directly and expressing the result in terms of unit vectors fixed in the IMU, as indicated by the transport theorem for vector differentiation[28].

3) Define joint positions, velocities, *and accelerations* (joint accelerations not included in standard method) in the 6 DOF kinematic model at time frame *i*+1 as the model state. The increase in number of unknowns resulting from adding joint accelerations to the state will be counteracted by an increase in number of equations produced by matching measured and integrated experimental IMU data.

4) To reduce the number of unknowns further, use numerical integration equations as additional constraints. These equations relate joint positions, velocities, and accelerations at time frames *i* to those at time frame *i*+1 such that joint accelerations are first time derivatives of corresponding joint velocities, and similarly for joint velocities and positions.

5) Find joint accelerations, velocities, and positions at time frame *i*+1 such that model IMU quantities at time frame *i*+1 match corresponding integrated, *measured, and differentiated* (last two not included in the standard method) experimental IMU quantities at time frame *i*+1 as closely as possible while satisfying numerical integration relationships.

6) Replace integrated, *measured, and differentiated* (last two not included in the standard method) experimental IMU quantities at time frame *i*+1 with corresponding model IMU quantities at time frame *i*+1 to minimize the effect of integration drift and prepare for solving the next time frame. This step projects the measured, integrated, and differentiated experimental IMU data onto the solution space of the kinematic model.

Given this overview of how both methods work, consider the number of equations, the number of unknowns, and their ratio for both methods applied to the 6 DOF walking model assuming measurements are available from either 4 or 2 IMUs (Table 3). While both methods are overdetermined when using all 4 IMUs (ratios > 1, 1.67 for standard method versus 2.67 for proposed method), our proposed method using only 2 IMUs is overdetermined by the same amount as the standard method using 4 IMUs (1.67 for proposed method with 2 IMUs and standard method with 4 IMUs). Furthermore, the standard method with only 2 IMUs is underdetermined (ratio = 0.83 < 1). While the standard method can still estimate joint positions and velocities when the problem is underdetermined, the solution is not unique, so the estimated joint kinematics will drift away from the actual joint kinematics. Creation of underdetermined problems when some IMUs are removed is likely why existing methods use one IMU per body segment. Our proposed method remains overdetermined when 2 IMUs are removed from the model because we make full use of constraint equations available from our kinematic model, measured and differentiated IMU data, and constraints available from numerical integration relationships.

Table 3: Comparison of number of equations, number of unknowns, and their ratio for standard and proposed methods of calculating the motion of a planar 4 segment, 6 DOF walking model using either 4 (all 4 segments) or 2 (pelvis and foot segments only) IMUs.

	Standard		**Proposed**	
Equations	**4 IMUs**	**2 IMUs**	**4 IMUs**	**2 IMUs**
Measured IMU data	0	0	12	6
Integrated IMU data	20	10	20	10
Differentiated IMU data	0	0	4	2
Integration relationships	0	0	12	12
Total	*20*	*10*	*48*	*30*
Unknowns	**4 IMUs**	**2 IMUs**	**4 IMUs**	**2 IMUs**
Generalized coordinates	6	6	6	6
Generalized speeds	6	6	6	6
Generalized accelerations	0	0	6	6
Total	*12*	*12*	*18*	*18*
Ratio	***1.67***	***0.83***	***2.67***	***1.67***

To evaluate whether the theoretical information provided in Table 3 is correct, we solved the 6 DOF walking model problem using the standard method with 4 IMUs, the standard method with only 2 IMUs (pelvis and foot), and the proposed method with 2 IMUs. All quantities listed in the Equations section of Table 3 were treated as measurements to be matched in the unscented filter update phase. We derived the non-linear kinematic constraint equations for model IMU quantities as a function of the model's joint positions, velocities, and accelerations using Autolev symbolic manipulation software. We generated synthetic joint motion and IMU data using joint kinematics taken from published experimental walking data for a single gait cycle[22]. We added zero mean, Gaussian white noise to synthetic IMU positions (standard deviation of 0.5 cm), angular velocities (standard deviation of 0.1 deg/s), and linear accelerations (standard deviation of 8 milli-g) to emulate the effects of skin motion and IMU measurement

noise. IMU measurement noise values were taken from the specifications of the IMUs used by Dr. Besier's company. The standard method used an explicit second-order Adams-Bashforth integrator to calculate IMU positions, velocities, and orientations at the new time frame *i*+1 from noisy synthetic IMU measurements at time frame *i*, while the proposed method used an implicit second-order Heun integrator to calculate the same quantities at time frame *i*+1 from noisy synthetic IMU measurements at time frame *i*+1. For both methods, higher order integrators could be used to improve integration accuracy. We assumed an IMU sampling frequency of 100 Hz, which is the current real-time streaming frequency of the IMUs used by Dr. Besier's company. We implemented the solution process for both methods in Matlab (The Mathworks, Natick, MA) using a custom UF algorithm we developed specifically for this problem.

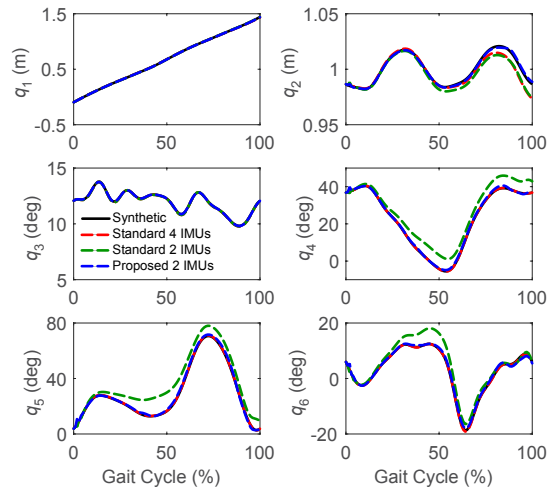

Fig. 2: Comparison of recovered joint positions for standard method with 4 IMUs and 2 IMUs and proposed method with 2 IMUs using noisy synthetic IMU data.

As shown in Fig. 2, our proposed method using 2 IMUs produced joint kinematics of comparable accuracy to those found by the standard method using 4 IMUs. As expected, the standard method with 2 IMUs performed worse than the other two methods. These findings are consistent with the theoretical assessment provided in Table 3 and are encouraging given that motion artifacts on the order of 0.5 cm would likely be excessive for an IMU attached to a shoe. For curiosity, we also used an optimization approach to re-solve the problem. While the results were similar, the optimization approach required a few seconds per time frame to solve, whereas our UF approach required only a fraction of a second.

3. Novel integration method for IMU-based motion measurement: (This section also contains confidential information that the University of Auckland requests not be released to persons outside the Government, except for purposes of review and evaluation.) For the third effort, PI Fregly has recently explored a novel way to integrate experimental IMU linear acceleration measurements *without* first removing the influence of gravity (henceforth called "gravity contamination"). Such an approach is potentially beneficial since it eliminates the use of imperfect IMU orientation information in the linear acceleration integration process, which could improve the solution accuracy of the entire motion estimation algorithm. At a high level, the approach eliminates the need to re-express IMU linear acceleration measurements in terms of unit vectors fixed in the inertial reference so that gravity can be subtracted prior to performing numerical integration. Instead, gravity-contaminated IMU linear acceleration measurements are numerically integrated directly, still expressed in terms of unit vectors fixed in the IMU, and the corresponding model linear kinematic quantities are gravity contaminated in a consistent manner for comparison.

This new integration approach is the natural result of viewing the numerical integration process from a vector rather than scalar perspective. After re-expressing IMU acceleration measurements in terms of *unit vectors fixed in the inertial reference frame* (which requires knowledge of IMU orientation) and subtracting off gravity, "strapdown inertial integration" numerically integrates the scalar components of the corrected acceleration vector. The resulting integrated velocity and position are also expressed in terms of unit vectors fixed in the inertial reference frame. However, using vector differentiation and integration concepts[28], it is also possible to numerically integrate gravity-contaminated IMU accelerations expressed in terms of *unit vectors fixed in the IMU* to produce gravity-contaminated IMU velocities and positions, also expressed in terms of *unit vectors fixed in the IMU*.

To describe how this vector integration process works, we first define some necessary terminology. Let S represent any IMU with origin So and N represent the inertial reference frame with origin No. Right-handed mutually perpendicular basis vectors $\mathbf{s}_x$, $\mathbf{s}_y$, and $\mathbf{s}_z$ are fixed in S, and similarly basis vectors $\mathbf{n}_x$, $\mathbf{n}_y$, and $\mathbf{n}_z$ are fixed N. ${}^N\mathbf{a}^{So}$ is the acceleration of point So as viewed by an observer fixed in N, ${}^N\tilde{\mathbf{a}}^{So}$ is the corresponding gravity-contaminated acceleration measured by the IMU, and similarly for velocity

${}^{N}\mathbf{v}^{So}$, gravity-contaminated velocity ${}^{N}\tilde{\mathbf{v}}^{So}$, position vector $\mathbf{p}^{NoSo}$ from No to So, and gravity-contaminated position vector $\tilde{\mathbf{p}}^{NoSo}$. In addition, ${}^{N}\boldsymbol{\omega}^{S}$ is the angular velocity of S in N as measured by the IMU. Each of these quantities is assumed to be expressed in terms of basis vectors fixed in S, making it unclear how numerical integration can be performed from the perspective of an observer fixed in reference frame N.

To find ${}^{N}\tilde{\mathbf{v}}^{So} = \tilde{v}_x\mathbf{s}_x + \tilde{v}_y\mathbf{s}_y + \tilde{v}_z\mathbf{s}_z$ and $\tilde{\mathbf{p}}^{NoSo} = \tilde{p}_x\mathbf{s}_x + \tilde{p}_y\mathbf{s}_y + \tilde{p}_z\mathbf{s}_z$ via numerical integration, we must first calculate $\dot{\tilde{v}} = [\dot{\tilde{v}}_x\ \dot{\tilde{v}}_y\ \dot{\tilde{v}}_z]$ and $\dot{\tilde{p}} = [\dot{\tilde{p}}_x\ \dot{\tilde{p}}_y\ \dot{\tilde{p}}_z]$ from the available data. Using the mathematical notation ${}^{N}d\mathbf{b}/dt$ to define time differentiation of any vector $\mathbf{b}$ as viewed by an observed fixed in N, we can apply the transport theorem for vector differentiation[28] to ${}^{N}\tilde{\mathbf{v}}^{So}$ to obtain the following vector relationships:

$$
\begin{aligned}
{}^{N}\tilde{\mathbf{a}}^{So} &= \frac{{}^{N}d\,{}^{N}\tilde{\mathbf{v}}^{So}}{dt} = \frac{{}^{S}d\,{}^{N}\tilde{\mathbf{v}}^{So}}{dt} + {}^{N}\boldsymbol{\omega}^{S} \times {}^{N}\tilde{\mathbf{v}}^{So} \\
&= \dot{\tilde{v}}_x\mathbf{s}_x + \dot{\tilde{v}}_y\mathbf{s}_y + \dot{\tilde{v}}_z\mathbf{s}_z + (\omega_y\tilde{v}_z - \omega_z\tilde{v}_y)\mathbf{s}_x + (\omega_z\tilde{v}_x - \omega_x\tilde{v}_z)\mathbf{s}_y + (\omega_x\tilde{v}_y - \omega_y\tilde{v}_x)\mathbf{s}_z \\
&= \tilde{a}_x\mathbf{s}_x + \tilde{a}_y\mathbf{s}_y + \tilde{a}_z\mathbf{s}_z
\end{aligned}
$$

Taking dot products in the $\mathbf{s}_x$, $\mathbf{s}_y$, and $\mathbf{s}_z$ directions, the three resulting scalar equations can be re-arranged to produce

$$
\begin{aligned}
\dot{\tilde{v}}_x &= \tilde{a}_x + (\omega_z\tilde{v}_y - \omega_y\tilde{v}_z) \\
\dot{\tilde{v}}_y &= \tilde{a}_y + (\omega_x\tilde{v}_z - \omega_z\tilde{v}_x) \\
\dot{\tilde{v}}_z &= \tilde{a}_z + (\omega_y\tilde{v}_x - \omega_x\tilde{v}_y)
\end{aligned}
$$

Following a similar process, we can also form

$$
\begin{aligned}
\dot{\tilde{p}}_x &= \tilde{v}_x + (\omega_z\tilde{p}_y - \omega_y\tilde{p}_z) \\
\dot{\tilde{p}}_y &= \tilde{v}_y + (\omega_x\tilde{p}_z - \omega_z\tilde{p}_x) \\
\dot{\tilde{p}}_z &= \tilde{v}_z + (\omega_y\tilde{p}_x - \omega_x\tilde{p}_y)
\end{aligned}
$$

To numerically integrate these two sets of first order ODEs, we require IMU measurements $\tilde{a} = [\tilde{a}_x\ \tilde{a}_y\ \tilde{a}_z]$ and $\omega = [\omega_x\ \omega_y\ \omega_z]$ at the current time point (i.e., the end of the integration interval) along with an implicit numerical integration scheme. An implicit scheme is needed since knowledge of $\tilde{v} = [\tilde{v}_x\ \tilde{v}_y\ \tilde{v}_z]$ at the current time point is needed to calculate $\dot{\tilde{v}} = [\dot{\tilde{v}}_x\ \dot{\tilde{v}}_y\ \dot{\tilde{v}}_z]$ at the current time point (and similarly for the position ODEs). An initial estimate of $\tilde{v}$ at the current time point is generated by taking an explicit numerical integration step (e.g., explicit Euler method) using knowledge of $\tilde{v}$ from the model at one or more previous time points, depending on the desired integration accuracy. Once a solution for $\tilde{v}$ has been generated, the process is repeated to find $\tilde{p} = [\tilde{p}_x\ \tilde{p}_y\ \tilde{p}_z]$ at the current time point.

Table 4: Relationship between gravity-contaminated linear kinematic quantities (indicated by tildes) and gravity-free linear kinematic quantities. Boldface type indicates a vector quantity, and all derivatives are vector derivatives where the observer is fixed in the inertial reference frame N.

$\tilde{\mathbf{p}}^{NoSo} = \mathbf{p}^{NoSo} - \frac{1}{2}gt^2\mathbf{n}_y$ $= p_x\mathbf{s}_x + p_y\mathbf{s}_y + p_z\mathbf{s}_z - \frac{1}{2}gt^2\mathbf{n}_y$ $= \tilde{p}_x\mathbf{s}_x + \tilde{p}_y\mathbf{s}_y + \tilde{p}_z\mathbf{s}_z$	${}^{N}\tilde{\mathbf{v}}^{So} = \frac{{}^{N}d\tilde{\mathbf{p}}^{NoSo}}{dt} = \frac{{}^{N}d\mathbf{p}^{NoSo}}{dt} - \frac{{}^{N}d\,\frac{1}{2}gt^2\mathbf{n}_y}{dt}$ $= {}^{N}\mathbf{v}^{So} - gt\mathbf{n}_y$ $= v_x\mathbf{s}_x + v_y\mathbf{s}_y + v_z\mathbf{s}_z - gt\mathbf{n}_y$ $= \tilde{v}_x\mathbf{s}_x + \tilde{v}_y\mathbf{s}_y + \tilde{v}_z\mathbf{s}_z$	${}^{N}\tilde{\mathbf{a}}^{So} = \frac{{}^{N}d\,{}^{N}\tilde{\mathbf{v}}^{So}}{dt} = \frac{{}^{N}d\,{}^{N}\mathbf{v}^{So}}{dt} - \frac{{}^{N}dgt\mathbf{n}_y}{dt}$ $= {}^{N}\mathbf{a}^{So} - g\mathbf{n}_y$ $= a_x\mathbf{s}_x + a_y\mathbf{s}_y + a_z\mathbf{s}_z - g\mathbf{n}_y$ $= \tilde{a}_x\mathbf{s}_x + \tilde{a}_y\mathbf{s}_y + \tilde{a}_z\mathbf{s}_z$

Once ${}^{N}\tilde{\mathbf{a}}^{So}$, ${}^{N}\tilde{\mathbf{v}}^{So}$, and $\tilde{\mathbf{p}}^{NoSo}$ are available at the current time point for all experimental IMUs, corresponding gravity-contaminated linear kinematic quantities are calculated for each model IMU. To perform these calculations, we input the current guess for the model state into the model, calculate the gravity-free linear acceleration, velocity, and position of each model IMU, contaminate those calculations with the influence of gravity as shown in Table 4, and finally express the resulting quantities in terms of basis vectors fixed in each model IMU. To avoid build up of integration errors related to gravity contamination, we apply gravity contamination to model IMU calculations and experimental IMU integration assuming time equals zero at the start of each integration interval. Differences between experimental and model gravity-contaminated quantities can then be used as errors when estimating the model state, *with no experimental IMU orientation information being required in the process*.

To explore whether this novel approach for integrating gravity-corrupted IMU acceleration data will work, we developed a simple 1 DOF inverted pendulum model containing a single IMU and drove the model through a prescribed cosine motion in Matlab. We numerically integrated the gravity-contaminated IMU linear acceleration data to find gravity-contaminated IMU velocity and position data, as described above. We then used the known time history of the model state (including joint acceleration) to calculate the corresponding model IMU linear kinematic quantities and contaminated them with gravity based on the equations in Table 4. The two sets of linear kinematic results were identical to within small expected numerical differences, demonstrating that this approach is worth exploring within our larger IMU-based motion measurement algorithm.

D. Simultaneous IMU- and marker-based motion measurement: In July of 2016, the PI and co-PI participated in a collaborative experimental session involving simultaneous collection of IMU and surface marker data from a healthy subject performing a wide range of activities, including walking, jumping, stair climbing, and running (Fig. 3). Drs. Fregly and Besier orchestrated the test session, and Dr. Besier provided the necessary IMUs through his company IMeasureU. The surface marker protocol was identical to the one used by Drs. Fregly and Besier on their recent NIH-funded "Grand Challenge Competition to Predict In Vivo Knee Loads"[29]. Data were collected from 13 IMUs placed on both feet, both shanks, both thighs, the front and back of the pelvis, the torso, both arms, and both wrists. Each IMU had three reflective markers placed on it to permit creation of marker-based IMU coordinate systems, which will be used for registering IMU positions and orientations to the marker data and a subsequent full-body kinematic walking model. IMU and marker data were synchronized using a common synchronization pulse delivered at the start and end of the test session. Prior to performing activity trials, the subject performed isolated ankle, knee, and hip motion trials for calibrating lower body joint positions and orientations in a full-body kinematic walking model. This data set will provide the foundation for developing the proposed IMU-based motion measurement algorithm.

Fig. 3: Combined IMU and surface marker motion capture session. Three surface markers were placed on each IMU to facilitate registration of IMUs to their associated body segments.

V. Results from Prior NSF Support

B.J. Fregly (PI) - Grant number CBET 1404767, $499,994, 8/15/14-7/31/17
CDS&E: A Next-Generation Computation Framework for Predicting Optimal Walking Motion
Summary of Results: For this project, the PI and colleagues developed EMG-driven leg models and a synergy-controlled subject-specific full-body walking model that successfully predicted how an individual post-stroke walked at his fastest comfortable speed given marker motion, ground reaction, and muscle EMG data for how he walked at his slower self-selected speed[25,30].
Intellectual Merit: The intellectual merit of this project was development of optimal control methods that can successfully calibrate subject-specific neuromechanical movement models to a wide range of disparate experimental movement data and successfully predict how a subject will move under new conditions for which no experimental data exist.
Broader Impacts: The broader impact of this project is development of computational modeling and simulation methods that can add objectivity to the design of neurorehabilitation treatments for stroke. Objective prediction of the best walking pattern a patient is theoretically capable of achieving could provide clinicians with valuable new information to improve the efficacy of the treatment design process.
Publications: References [25,30–39].
Evidence of Research Products: This project has resulted in 9 journal publications thus far, with 3 more currently in review and 1 more being completed. In addition, the project provided an international workshop to help train the musculoskeletal modeling research community on how to use the optimal

control methods developed for the project. All data, models, and Matlab code generated by the project have been made publically available on Simtk.org.

Thor Besier (co-PI) – No prior NSF support.

VI. Plan of Work

A. Research Overview

The ultimate goal of this project is to develop a wireless user-friendly IMU-based motion measurement system that is so simple and easy to use that virtually any patient or caregiver can use it to measure full-body walking movements at home or in the community with little training. Such a system could be clinically beneficial for both remote assessment of patient function using logged data and remote delivery of rehabilitation prescriptions using real-time feedback. At the core of the proposed system will be a novel motion estimation algorithm that will work for data logging and real-time applications. To make the system as simple and easy to use as possible, the algorithm will require only 6 IMUs to measure full-body walking kinematics, where each IMU is attached to the body easily and repeatably. The proposed project will progress in three phases. **Phase 1** will involve algorithm development. **Phase 2** will involve algorithm evaluation for off-line applications. **Phase 3** will involve algorithm deployment for real-time applications. All coding for phases 1 and 2 will be done in Matlab, while for Phase 3, C/C++ will be used to improve computational speed. For phase 3, we emphasize that our goal is *not* to explore the effectiveness of different types of real-time feedback but rather simply to demonstrate that the final system is capable of calculating full-body joint kinematics in real time for future real-time feedback applications.

Our proposed IMU-based motion estimation algorithm possesses a number of novel technical aspects that potentially make it more flexible, easier to use, and more accurate than existing algorithms:

- Kinematic model matching of IMU linear and angular position/velocity/acceleration data, not just linear position/velocity and angular velocity data – this aspect increases the number of unknowns.
- Enforcement of model kinematic constraints relating IMU data to model generalized coordinates and their first two time derivatives – this aspect provides more equations.
- Enforcement of numerical integration relationships between joint positions, velocities, and accelerations – this aspect also provides more equations.
- Use of IMU data at current time point to estimate model kinematics at that time point – most recent IMU data are used to estimate model kinematics, potentially improving motion measurement accuracy.
- Numerical integration of measured IMU linear acceleration data directly without gravity correction – potentially improves motion measurement accuracy.
- Elimination of magnetometer data from the motion estimation process – these data are the least reliable and can slow the sampling rate of the accelerometer and gyroscope data.
- Estimation of static body poses without knowing experimental IMU orientations - gravity-contaminated linear accelerations from model IMUs act like strings controlling the body segments of a puppet.

B. Research Details

Given the ultimate goal described above, we propose a three-phase approach for developing and evaluating our proposed IMU-based motion estimation algorithm and deploying it in a wireless system for real-time applications. Though developed specifically to estimate full-body joint kinematics during walking, the proposed algorithm should work equally well for other tasks (e.g., stair climbing, rising from a chair) and other human body models (e.g., pelvis and lower body, torso and upper body). Measurement of walking creates a well-defined scope for the kinematic models and experimental data used for algorithm development and testing. For all phases of the project, 9-axis wireless IMUs from by Dr. Besier's company IMeasureU will provide the necessary experimental IMU data collected at 100 Hz, where the 3-axes of magnetometer data will be ignored.

Phase 1. Algorithm Development: Our proposed IMU-based motion measurement algorithm will be an expanded version of the unscented filter (UF) algorithm we developed for our preliminary study involving the planar 6 DOF walking model (Fig. 1). Below we describe the process we will follow to develop and test the proposed algorithm.

The first task for our algorithm development process will be to make our existing UF algorithm more

general and flexible. To begin, we will modify the algorithm so that it can accommodate a larger number of model generalized coordinates, which should not be difficult. Next, we will extend to three-dimensional (3D) space the way we perform multistep implicit numerical integration of measured experimental IMU angular velocities to obtain integrated experimental IMU orientations. To avoid the well-known problem of gimbal lock, we will use quaternions to represent the 3D orientation of each IMU in the inertial reference frame. The first time derivative of the redundant set of four quaternions will be written as a function of the values of the four quaternions plus the values of the three angular velocity components expressed in terms of unit vectors fixed in the IMU[40], which is perfect since measured experimental IMU angular velocities are already expressed in this way. The resulting quaternions will be converted into rotation matrices from which traditional Euler angles will be extracted. The orientation of each model IMU with respect to the laboratory reference frame will be expressed in terms of the same Euler angles for error calculation purposes. Furthermore, we will incorporate expanded numerical integration and differentiation options for experimental IMU measurements so that model data from more than one past time point can be used to improve numerical accuracy (e.g., multi-step implicit numerical integration). In addition, we will add joint jerk (one time derivative higher than acceleration) to the state vector, since estimating a state derivative (i.e., acceleration derivative) at least one degree higher than our highest desired state (i.e., acceleration) improves the accuracy of the desired state estimates[21]. Finally, we will add *parameter estimation* to the *state estimation* capabilities of our existing UF so that calibration of constant model parameter values representing the positions/orientations of the IMUs and joints in the body segments can be accommodated. To prevent large changes in joint or IMU position/orientation parameters that would produce little improvement in matching of IMU data, our UF algorithm will penalize parameter changes greater than specified values, as this approach worked well in our previous work finding joint parameters via optimization methods[24].

The UF algorithm development process will require extensive testing using experimental walking data and a kinematic walking model representative of real-life conditions. The necessary walking data will be taken from our preliminary study described above in which IMU- and marker-based motion capture data were collected simultaneously from a single healthy subject. The necessary walking model will be taken from a parametric 29 DOF full-body model we developed previously in Autolev and have used extensively for inverse kinematic, inverse dynamic, and predictive walking optimization studies[11,22–24,41–44]. The base segment of the model is the pelvis, which is connected to the inertial reference frame via a 6 DOF joint. For the lower body, the hips are modeled as 3 DOF ball-and-socket joints, the knees as 1 DOF pin joints, and the ankles as 2 DOF non-intersecting pin joints. For the upper body, the lower back is modeled as a 3 DOF ball-and-socket joint, the shoulders as 3 DOF ball-and-socket joints, and the elbows as 1 DOF pin joints. A more complex shoulder model is not needed for this project since scapular motion is minimal during walking, allowing excellent tracking of surface marker positions using our current 29 DOF walking model[22,24]. Since we developed our model in Autolev, we have full access to the kinematic equations and full control over their derivation. By making wise modeling choices and exporting the final equations as C code, we will create highly efficient equations for real-time applications. Since Dr. Ton van den Bogert at Cleveland State University has used Autolev to generate three-dimensional skeletal dynamic equations that can be evaluated in real time[45–47], we are confident that less complex three-dimensional skeletal kinematic equations generated by Autolev can also be evaluated in real time.

Using our existing data set and our 29 DOF walking model, we will follow the three-step algorithm development process outlined below that we have used successfully in the past[11]:

Step 1) Synthetic data without noise. We will start by developing and testing the proposed algorithm using synthetic IMU data without noise, where the synthetic data will be generated using the results of a marker-based inverse kinematic analysis performed with our 29 DOF walking model. Synthetic joint kinematics (positions, velocities, and accelerations) will be found by fitting joint positions from inverse kinematics using polynomial-Fourier regression, as we have done previously[22]. Once synthetic joint kinematics are calculated, we will input them into the 29 DOF walking model to calculate synthetic angular velocities and linear accelerations for the model IMUs, expressed in terms of unit vectors fixed in each IMU. The acceleration due to gravity will be added to the synthetic linear acceleration of each model IMU. Synthetic IMU data will be generated for a sampling rate of 100 Hz, which is the sampling rate used

by IMeasureU for real-time applications. A marker-based inverse kinematic analysis of an initial standing static trial, where body segment as well as IMU marker locations were measured, will be used to determine model IMU positions and orientations on the body segments of the 29 DOF walking model.

Step 2) Synthetic data with noise. Once the proposed algorithm works well on synthetic IMU data without noise, we will repeat the testing process using synthetic IMU data with noise. These data will be generated by adding synthetic noise representing skin motion and IMU measurement errors to the synthetic IMU data. Specifically, zero mean, Gaussian white noise will be added to the three components of each model IMU position on its respective body segment (standard deviations between 0.25 and 1.0 cm in increments of 0.25 cm)[48], angular velocity (standard deviation of 0.1 deg/s), and linear acceleration (standard deviation of 8 milli-g), where IMU measurement noise values were taken from the specifications of the IMUs used by Dr. Besier's company.

Step 3) Experimental data. Once the proposed algorithm works well on synthetic IMU data with noise, we will repeat the testing process using the experimental IMU data. For this situation, there is no ground truth joint kinematic data against which to compare the calculated joint kinematics. For this reason, we will use joint kinematics calculated from marker-based inverse kinematic analyses for comparison. The goal will be to demonstrate that IMU-based joint translations/rotations are within a root-mean-square difference of 1 cm and 4 deg from marker-based results[8,11,49–51]. These values represent the uncertainties present in calculated joint translations/rotations due to soft tissue artifacts, errors in joint positions/orientations, and variability in surface marker placements when using a marker-based motion capture system. If our IMU-based motion estimation algorithm is able to measure joint kinematics to within the level of uncertainty of joint kinematics obtained from a marker-based motion capture system, then our algorithm should be applicable in any situation for which a traditional optical motion capture system would be used.

Within this three-step process, we will have two additional layers of complexity. The first layer will involve the number of IMUs. All algorithm development work will initially be performed using a full set of IMUs, with one IMU on every body segment in the 29 DOF walking model (12 IMUs total). Once the algorithm works well using all IMUs, we will reduce the number of IMUs down to a minimal set involving one IMU on each foot, one on the pelvis, one on the torso, and one on each wrist (6 IMUs total). We have performed the same equations/unknowns/ratio analysis for the 29 DOF walking model as we performed in Table 3 for the 6 DOF walking model. For the full set of IMUs, we will have 275 equations, 87 unknowns, and a ratio of 3.15, which is highly overdetermined. For the minimal set of IMUs, we will have 166 equations, 87 unknowns, and a ratio of 1.91, which is still highly overdetermined. Thus, it is theoretically possible to recover joint kinematics (including joint accelerations) in our 29 DOF walking model using data from only 6 IMUs. The same statement holds true for only the lower body portion of our 29 DOF walking model, where with only one IMU on the pelvis and one IMUs on each foot, the ratio of equations to unknowns is 1.67 – still overdetermined by a healthy amount.

The second layer of complexity involves calibration of IMU and joint parameters defining the positions and orientations of the IMUs and joints in the body segments of the 29 DOF walking model. All algorithm development work will initially be performed using IMU positions/orientations that are calculated using the locations of the surface markers placed on the IMUs, and joint positions/orientations that are calculated using our existing optimization procedure that operates on experimental marker data[11,22–24]. Once an algorithm works well using known model parameter values, we will add to the problem formulation parameter estimation for the constant parameters defining the positions/orientations of the IMUs and joints in the body segments. We will determine whether or not we can recover the correct values (for synthetic IMU data without and with noise) or values consistent with those obtained using the corresponding marker data (for experimental IMU data). Similar to what we have done in the past using marker data[22,24], we will calibrate model parameter values using IMU data by first performing isolated joint calibrations with data from isolated joint motion trials, and then performing a full-body calibration with data from one or more walking trials. Note that the UF algorithm already handles *parameter estimation* as well as *state estimation*.

Phase 2. Algorithm Evaluation: In the second phase of the project, we will evaluate the ease of use and associated accuracy of our proposed algorithm for off-line applications. To this end, we will have 10 healthy subjects collect their own IMU-based walking data, the goal being to demonstrate that with

minimal training, individuals in any environment can collect their own kinematic walking data using our algorithm. Prior to data collection, each subject will review a training worksheet and/or video that describes how and where to attach each of the 6 IMUs required for collecting full-body joint kinematics during walking. No researcher feedback will be provided on IMU placement or attachment. Subjects will wear their own sneakers with laces and their own exercise clothes. The training materials will instruct them on how to attach 1 IMU through the laces on the top of each sneaker, 1 IMU on waist in the small of the back using a provided belt, 1 IMU on each wrist using provided wrist bands, and 1 IMU on the torso using a provided chest strap similar to straps used for heart rate monitors. After a subject works through the training materials, he or she should be able to put on the IMUs and be ready for data collection within 3 minutes – much less time than required for marker-based motion capture. Each subject will be timed while putting on the IMUs to verify that we have achieved this desired minimal set-up time. At the end of data collection, subjects will provide input on how IMU attachment could be simplified further.

To evaluate kinematic accuracy when subjects don the IMUs themselves with minimal instruction, we will collect IMU and surface marker data simultaneously from each subject. Both types of data will be synchronized and collected wirelessly using a Vicon motion capture system (Oxford Metrics, Yarnton, Oxfordshire, UK). After the subject has attached the 6 IMUs to his or her body, the researchers will attach surface markers to the IMUs and the subject's body segments. Three surface markers will be attached to each IMU, and surface markers will be attached to each body segment using the full-body marker set employed by the PI for previous studies[11,22–25,29]. At this point, the subject will be instructed to perform random calibration motions described in the training materials, again without researcher feedback. These motions are intended to exercise each functional axis in the 29 DOF walking model. Following completion of the calibration motions, the subject will be instructed to walk back and forth across the lab, with IMU- and marker-based motion capture data being collected simultaneously. Collection of force plate data will not be necessary for this kinematic evaluation. Once 10 walking trials are collected at the subject's self-selected speed, the researchers will verbally and visually instruct the subject how to perform a sequence of isolated (rather than random) joint motion trials.

The collected IMU and marker data will be analyzed separately off-line and the joint kinematics and joint positions/orientations produced by each type of data will be compared. First, our UF algorithm will use IMU data from the random calibration motions to estimate model states as well as model parameters defining joint and IMU positions/orientations in the body segments. Similarly, our existing optimization algorithm will use surface marker data from the same motions to estimate model parameter values defining joint positions/orientations in the body segments. IMU positions/orientations in the body segments will be also calculated directly from the three surface markers attached to each IMU. The resulting joint and IMU positions/orientations produced from the two types of data will be compared to assess their level of similarity. Next, the joint and IMU position/orientation calibration process will be repeated for both types of data using the isolated joint motion trials and one representative walking trial analyzed together. The resulting parameter values will be compared with those produced by the random calibration motions to verify that random motions can be used for estimating model parameters. Finally, the calibrated kinematic model produced by each type of data will be used to estimate joint kinematics for each of the subject's 10 walking trials. For the IMU data, our UF algorithm will be used to estimate joint positions, velocities, and accelerations (model parameters fixed at their calibrated values), while for the surface marker data, standard inverse kinematic analyses will be used to estimate joint positions. The joint position time histories produced by both types of data will be compared, hopefully demonstrating that the differences are within the level of uncertainty in joint positions calculated using marker-based motion capture systems (see above). If larger differences are found, we will use those differences to identify aspects of our UF algorithm that require further refinement. If the joint position time histories from IMU data are within the level of uncertainty of the joint position time histories from surface marker data, we will have achieved our desired ease-of-use and accuracy goals for off-line applications.

Phase 3. Algorithm Deployment: In the final phase of the project, we will evaluate computational speed of our proposed algorithm when deployed on hardware for real-time applications. Again, the goal is not to evaluate any particular feedback methodology but rather simply to demonstrate that our proposed IMU-based motion measurement algorithm is fast enough computationally for future real-time applications.

To deploy our algorithm for real-time applications, we will develop a wireless IMU-based motion feedback system that consists of: 1) 6 miniature wireless IMUs, 2) a Windows tablet control unit, and 3) software for real-time calculation and display of joint angles during walking (Fig. 3). Wireless IMUs from IMeasureU (Fig. 3) will provide input signals to the IMU-based motion measurement algorithm. These IMUs currently connect to an iPhone, iPad, or PC using a Bluetooth Low Energy communication protocol, which is capable of transmitting synchronized accelerometer and gyroscope data from up to 14 sensors at 100 Hz. A Windows tablet will be used as a smart device control unit due to its computational horsepower, ability to act is a flat panel display, and ability to run Matlab or OpenSim[52] for real-time display of kinematic data. Furthermore, Windows tablets such as the Microsoft Surface Book 2 or the HP ZBook X2 possess Nvidia graphics cards with more than 500 GPUs capable of performing floating point calculations, which would make GPU-based parallel computing possible if desired or required. Custom software written in C will use the IMeasureU application programming interface to access raw IMU sensor data in real time. These data will be streamed to our UF algorithm (translated from Matlab into C) running on the Windows tablet for real-time calculation of joint angles in our 29 DOF walking model. The calculated joint angles will then be displayed in real time on the tablet using either animated plots created in Matlab or an animated skeleton displayed in OpenSim (again, the form of the feedback display is not important for this test).

To verify that our UF algorithm deployed to a Windows tablet is able to calculate and display joint kinematic data in real time during walking, we will have 3 additional subjects perform real-time data collection on themselves without simultaneous collection of marker-based motion capture data. The goal of these tests will be to verify that 1) individuals who review some simple training materials can don the IMUs and collect data by themselves, 2) the complete system can rapidly calibrate joint and IMU position/orientation parameters, and 3) the complete system can collect and display calculated joint positions in real time. Our goal will be to display joint position data within 75 ms of the data being collected by the IMUs, as a longer time delay reduces the usefulness of the data[53]. Similar to a recent study[54], POSIX timer functions will be used to calculate the amount of time expended from collection of data by the IMU to display of joint positions by the Windows tablet.

C. Research Issues and Workarounds

There are three categories of issues that we are most likely to encounter in this project. The first category is filter issues. For the unscented filter algorithm, the matrix square root decomposition step used to generate sigma points can occasionally cause a numerical stability issue. This issue arises when the state covariance matrix becomes non-positive definite, thereby preventing the matrix square root from being calculated. If this problem arises, we will implement a more complex square-root unscented filter (SRUF) in place of a standard UF. The SRUF is similar computationally to the UF but has improved numerical stability and guarantees positive semi-definiteness of the state covariance matrix[55]. In addition, if unmodeled accelerometer or gyroscope biases appear to be affecting the accuracy of our state estimates, we will investigate modeling these biases and adding them to our UF algorithm.

The second category is speed issues. Computational speed will only be a potential issue for the real-time tests performed in Phase 3. If porting our Phase 1 and 2 Matlab code to C/C++ in Phase 3 does not provide sufficient speed improvement for real-time display, we will explore using the 500+ GPUs on the Nvidia graphics card in the Windows tablet to parallelize the 29 DOF kinematic model calculations performed in the UF update stage.

The final category is drift issues. The addition of noise to the synthetic IMU data and the use of experimental IMU data will likely make IMU-based motion measurement more prone to integration drift, especially for the three translational DOFs. Since the goal of this project is not to solve all known issues with using IMU data to measure human movement, and since typical assessment or rehabilitation applications will be more interested in joint rotations than in joint translations, we will not expend a significant amount of time and effort attempting to eliminate integration drift from calculated joint translations. The use of highly redundant measurements and a kinematic model with joint constraints should naturally reduce the effects of integration drift, at least to the extent that data from all IMUs does not drift in the same direction. Nonetheless, we will still explore using two special conditions to provide information that can be used to correct integration drift. The first is when the foot is flat on the ground

during stance phase, which should be detectable using foot IMU data. In this situation, the foot IMU will be a known height above the floor, and this knowledge will be used to reset the superior-inferior translation of the pelvis. The second situation is when the subject is standing statically, which should be detectable by identifying when the magnitudes of all IMU angular velocity measurements are zero and the magnitudes of all IMU acceleration measurements are 9.8 m/s^2 to within some tolerance. In this situation, not only will the foot IMU be a known height above the floor, but also the angle between model and corresponding experimental IMU gravity-contaminated acceleration vectors should be zero, creating a reverse "puppet-like" situation for adjusting model generalized coordinates.

For future application of the proposed system to clinical populations, some patients may not be able to perform the joint ranges of motion required for calibration of kinematic model joint parameters – a problem faced by optical motion capture systems as well. Though beyond the scope of the present project, such situations could potentially be addressed by using statistical shape modeling software such as the Musculoskeletal Atlas Project[56] directed by the co-PI to generate kinematic models that provide reasonable representations of individual patients.

D. Education Overview

Two educational activities will be integrated with the research undertaken for this project: 1) recruitment of minority and female students for involvement in the research, and 2) an international Olympiad between economically disadvantaged middle school students in Houston and middle school students in Auckland.

E. Education Details

1. Research Involvement for Minority and Female Students (Years 1 through 3): The PI will use his undergraduate courses in Dynamics and Musculoskeletal Modeling, as well as Rice residential college interactions, as avenues for recruiting minority and female students for research involvement.

Recruitment of Undergraduate Researchers. Recruitment will involve identifying minority and female students interested in research and inviting them to participate in lab meetings and mentored undergraduate research projects. Using this approach, the PI has successfully recruited minority and female undergraduates for research involvement from past classes.

Leveraging Support Mechanisms. The PI will seek REU supplements and funding from programs at Rice – for instance, the Brown Undergraduate Research Internship Program and Century Scholars Program – to financially support undergraduate research on the project.

Independent Research Projects. Specific projects available to undergraduates will include processing and analyzing IMU- and marker-based motion capture data and evaluating the performance of the IMU-based motion estimation algorithm. Undergraduate researchers will keep laboratory notebooks, prepare oral and written reports, and participate in university and national conferences as appropriate.

2. International Olympiad between Middle School Students in the U.S. and New Zealand (Years 1 through 3): In addition, we will organize an annual international "Jump Off" Olympiad between economically disadvantaged middle school students in Houston, TX and middle schools students in Auckland, New Zealand. Baylor College of Medicine Academy at James D. Ryan (Baylor@Ryan) Middle School is not far from the Rice University campus. Baylor@Ryan is part of the Houston public school system, is located in the low income Greater Third Ward, and serves underrepresented groups, with a 35% African-American and 45% Hispanic student population. Each year of the project, students from Baylor@Ryan and Belmont Intermediate School in Auckland will participate in a live "Jump Off" via Skype. A week prior to the "Jump Off," students in both schools will learn about each other and the other country. During the actual competition, students from both schools will be invited in pairs to strap on a belt-mounted IMeasureU IMU. The two students will jump as high as they can, and IMeasureU's Jump app installed on an iPhone will calculate each student's jump height. The boy and girl from each country who jump the highest will each receive a Fitbit activity tracker as a prize. The boys' and girls' teams with the largest sum of best four jump heights will be designated the Olympiad winner for that year. PI Fregly and co-PI Besier will alternate years giving a brief "chalk talk" at the end on how the IMeasureU iPhone app calculates jump height using the belt-mounted IMU. Auckland is 18 hours ahead of Houston, so the end of the school day in Houston matches well with the start of the school day in Auckland.

E. REFERENCES CITED

1. Murphy L., Bolen J., Helmick C.G., and Brady T.J. (2009) Comorbidities are very common among people with arthritis. In: *Proceedings of the 20th National Conference on Chronic Disease Prevention and Control*. National Harbor, MD:Poster 43.
2. Praemer, A., Furner, S., Rice D.P. (1999) *Musculoskeletal Conditions in the United States*. American Academy of Orthopaedic Surgeons, Rosemont, IL.
3. Arthritis Foundation (2016) Osteoarthritis Fact Sheet. *http://www.arthritis.org/files/images/AF_Connect/Departments/Public_Relations/Osteoarthritis-fact-sheet-from-AF-Final-3* .
4. National Stroke Association (2016) Stroke Fact Sheets. *http://www.stroke.org/site/PageServer?pagename=factsheets* .
5. National Parkinson Foundation (2016) Parkinson's Disease Overview. *http://www.parkinson.org/parkinson-s-disease.aspx* .
6. tates R.A., Pappas E., and Salem Y. (2009) Overground physical therapy gait training for chronic stroke patients with mobility deficits. *The Cochrane Database of Systematic Reviews* **3**, CD006075.
7. Bogey R. and Hornby G.T. Gait training strategies utilized in poststroke rehabilitation: are we really making a difference? *Topics in Stroke Rehabilitation* **14**, 1–8.
8. Koning B.H.W., van der Krogt M.M., Baten C.T.M., and Koopman B.F.J.M. (2015) Driving a musculoskeletal model with inertial and magnetic measurement units. *Computer Methods in Biomechanics and Biomedical Engineering* **18**, 1003–1013.
9. Roetenberg D., Luinge H., and Slycke P. (2013) *Xsens MVN: Full 6DOF human motion tracking using miniature inertial sensors*.
10. Perception Neuron Corporation Home Page (2017) https://neuronmocap.com/.
11. Reinbolt J.A., Schutte J.F., Fregly B.J., Koh B. Il, Haftka R.T., George A.D., and Mitchell K.H. (2005) Determination of patient-specific multi-joint kinematic models through two-level optimization. *Journal of Biomechanics* **38**, 621–626.
12. Kortier H.G., Sluiter V.I., Roetenberg D., and Veltink P.H. (2014) Assessment of hand kinematics using inertial and magnetic sensors. *Journal of Neuroengineering and Rehabilitation* **11**, 70.
13. El-Gohary M. and McNames J. (2012) Shoulder and elbow joint angle tracking with inertial sensors. *IEEE Transactions on Biomedical Engineering* **59**, 2635–2641.
14. Bonnet V., Ramdani S., Azevedo-Coste C., Fraisse P., Mazzà C., and Cappozzo A. (2013) Integration of human walking gyroscopic data using empirical mode decomposition. *Sensors* **14**, 370–81.
15. Schiefer C., Ellegast R.P., Hermanns I., Kraus T., Ochsmann E., Larue C., and Plamondon A. (2014) Optimization of inertial sensor-based motion capturing for magnetically distorted field applications. *Journal of Biomechanical Engineering* **136**, 121008.
16. Fattey M.G. and Fregly B.J. (2008) Simultaneous determination of skeletal model parameter values, motions, and controls from noisy measurement data. In: *Proceedings of the ASME Summer Bioengineering Conference*. Marco Island, FL:SBC2008-192605.
17. Julier S.J., Uhlmann J.K., and Durrant-Whyte H.F. (1995) A new approach for filtering nonlinear systems. In: *Proceedings of the American Control Conference*. Seattle, WA:1628–1632.
18. Julier S.J. and Uhlmann J.K. (1997) New extension of the Kalman filter to nonlinear systems. In: *Proceedings of the SPIE Signal Processing, Sensor Fusion, and Target Recognition VI Conference*. Orlando, FL:3068, 182–193.
19. Wan E.A., Van Der Merwe R., and Nelson A.T. (2000) Dual estimation and the unscented transformation. *Neural Information Processing Systems* **12**, 666–672.
20. Wan E.A. and Van Der Merwe R. (2001) The unscented Kalman filter. In: *Kalman Filtering and Neural Networks*.:221–280.
21. Crassidis J.L. and Junkins J.L. (2004) *Optimal Estimation of Dynamic Systems*. 1st editio. Chapman & Hall/CRC Press, Boca Raton, FL.

22. Fregly B.J., Reinbolt J.A., Rooney K.L., Mitchell K.H., and Chmielewski T.L. (2007) Design of patient-specific gait modifications for knee osteoarthritis rehabilitation. *IEEE Transactions on Biomedical Engineering* **54**, 1687–1695.
23. Reinbolt J.A., Haftka R.T., Chmielewski T.L., and Fregly B.J. (2007) Are patient-specific joint and inertial parameters necessary for accurate inverse dynamics analyses of gait? *IEEE Transactions on Biomedical Engineering* **54**, 782–793.
24. Reinbolt J.A., Haftka R.T., Chmielewski T.L., and Fregly B.J. (2008) A computational framework to predict post-treatment outcome for gait-related disorders. *Medical Engineering & Physics* **30**, 434–443.
25. Meyer A.J., Eskinazi I., Jackson J.N., Rao A.V., Patten C., and Fregly B.J. (2016) Muscle synergies facilitate computational prediction of subject-specific walking motions. *Frontiers in Bioengineering and Biotechnology* **4**, 77.
26. Woodman O.J. (2007) *An Introduction to Inertial Navigation*. Cambridge, England
27. Chapra S.C. and Canale, Raymond P. (2006) *Numerical Methods for Engineers*. McGraw-Hill, New York.
28. Kane T.R. and Levinson D.A. (1985) *Dynamics: Theory and Applications*. McGraw-Hill, New York.
29. Fregly B.J., Besier T.F., Lloyd D.G., Delp S.L., Banks S.A., Pandy M.G., and D'Lima D.D. (2012) Grand challenge competition to predict in vivo knee loads. *Journal of Orthopaedic Research* **30**, 503–513.
30. Meyer A.J., Patten C., and Fregly B.J. (2017) Lower extremity EMG-driven modeling of walking with automated adjustment of musculoskeletal geometry. *PLoS ONE* **12**.
31. De Groote F., Kinney A.L., Rao A.V., and Fregly B.J. (2016) Evaluation of direct collocation optimal control problem formulations for solving the muscle redundancy problem. *Annals of Biomedical Engineering* **44**, 2922–2236.
32. Eskinazi I. and Fregly B.J. (2013) Surrogate knee contact modeling using artificial neural networks. In: *ASME Summer Bioengineering Conference*. June 26-29, Sunriver, OR.
33. Eskinazi I. and Fregly B.J. (2017) A computational framework for simultaneous estimation of muscle and joint contact forces and body motion using optimization and surrogate modeling. *Medical Engineering & Physics* (in revision).
34. Liu F., Hager W.W., and Rao A. V. Adaptive mesh refinement method for optimal control using decay rates of Legendre polynomial coefficients. *IEEE Transactions on Control Systems Technology* (in revision).
35. Weinstein M.J. and Rao A.V. (2017) Algorithm: ADiGator, a toolbox for algorithmic differentiation of mathematical functions in MATLAB using source transformation via operator overloading. *ACM Transactions on Mathematical Software* (in press).
36. Weinstein M.J. and Rao A. V. (2016) A source transformation via operator overloading method for the automatic differentiation of mathematical functions in MATLAB. *ACM Transactions on Mathematical Software* **42**, 11:1-11:44.
37. Hager W.W., Hou H., and Rao A. V. (2016) Lebesgue constants arising in a class of collocation methods. *IMA Journal of Numerical Analysis* (in review).
38. Liu F., Hager W.W., and Rao A.V. (2016) Adaptive mesh refinement for optimal control using nonsmoothness detection and mesh size reduction. *Journal of the Franklin Institute* **352**, 4081–4106.
39. Hager W.W., Hou H., Mohapatra S., and Rao A.V. (2017) Convergence rate for an hp collocation method applied to unconstrained optimal control. *Numerische Mathematik* (in review).
40. Kane T.R., Likins P.W., and Levinson D.A. (1983) *Spacecraft Dynamics*. McGraw-Hill, New York.
41. Koh B.-I., Reinbolt J.A., George A.D., Haftka R.T., and Fregly B.J. (2009) Limitations of parallel global optimization for large-scale human movement problems. *Medical Engineering & Physics* **31**, 515–521.
42. Fregly B.J., Reinbolt J.A., and Chmielewski T.L. (2008) Evaluation of a patient-specific cost function to predict the influence of foot path on the knee adduction torque during gait. *Computer Methods in Biomechanics and Biomedical Engineering* **11**, 63–71.

43. Koh B. Il, Reinbolt J.A., Fregly B.J., and George A.D. (2004) Evaluation of parallel decomposition methods for biomechanical optimizations. *Computer Methods in Biomechanics and Biomedical Engineering* **7**, 215–225.
44. Fregly B.J. (2008) Computational assessment of combinations of gait modifications for knee osteoarthritis rehabilitation. *IEEE Transactions on Biomedical Engineering* **55**, 2104–2106.
45. van den Bogert A.J., Blana D., and Heinrich D. (2011) Implicit methods for efficient musculoskeletal simulation and optimal control. *Procedia IUTAM* **2**, 297–316.
46. van den Bogert A.J., Geijtenbeek T., Even-Zohar O., Steenbrink F., and Hardin E.C. (2013) A real-time system for biomechanical analysis of human movement and muscle function. *Medical & Biological Engineering & Computing* **51**, 1069–1077.
47. Chadwick E.K., Blana D., Kirsch R.F., and van den Bogert A.J. (2014) Real-time simulation of three-dimensional shoulder girdle and arm dynamics. *IEEE Transactions on Biomedical Engineering* **61**, 1947–1956.
48. ackson J.N., Hass C.J., and Fregly B.J. (2015) Residual elimination algorithm enhancements to improve foot motion tracking during forward dynamic simulations of gait. *Journal of Biomechanical Engineering* **137**, 111002.
49. Fiorentino N.M., Atkins P.R., Kutschke M.J., Goebel J.M., Foreman K.B., and Anderson A.E. (2017) Soft tissue artifact causes significant errors in the calculation of joint angles and range of motion at the hip. *Gait and Posture* **55**, 184–190.
50. Reinschmidt C., van den Bogert A.J., Lundberg A., Nigg B.M., Murphy N., Stacoff A., and Stano A. (1997) Tibiofemoral and tibiocalcaneal motion during walking: external vs. skeletal markers. *Gait and Posture* **6**, 98–109.
51. Besier T.F., Sturnieks D.L., Alderson J.A., and Lloyd D.G. (2003) Repeatability of gait data using a functional hip joint centre and a mean helical knee axis. *Journal of Biomechanics* **36**, 1159–1168.
52. Delp S.L., Anderson F.C., Arnold A.S., Loan P., Habib A., John C.T., Guendelman E., and Thelen D.G. (2007) OpenSim: open-source software to create and analyze dynamic simulations of movement. *IEEE Transactions on Biomedical Engineering* **54**, 1940–1950.
53. Kannape O.A. and Blanke O. (2013) Self in motion: sensorimotor and cognitive mechanisms in gait agency. *Journal of Neurophysiology* **110**, 1837–1847.
54. Pizzolato C., Reggiani M., Modenese L., and Lloyd D.G. (2017) Real-time inverse kinematics and inverse dynamics for lower limb applications using OpenSim. *Computer Methods in Biomechanics and Biomedical Engineering* **20**, 436–445.
55. Van Der Merwe R. and Wan E.A. (2001) The square-root unscented Kalman filter for state and parameter-estimation. In: *Proceedings of the International Conference on Acoustics, Speech, and Signal Processing*. Salt Lake City, UT:3461–3464.
56. Zhang J., Fernandez J., Hislop-Jambrich J., and Besier T.F. (2016) Lower limb estimation from sparse landmarks using an articulated shape model. *Journal of Biomechanics* **49**, 3875–3881.